

JAAS

Accepted Manuscript



This is an *Accepted Manuscript*, which has been through the Royal Society of Chemistry peer review process and has been accepted for publication.

Accepted Manuscripts are published online shortly after acceptance, before technical editing, formatting and proof reading. Using this free service, authors can make their results available to the community, in citable form, before we publish the edited article. We will replace this *Accepted Manuscript* with the edited and formatted *Advance Article* as soon as it is available.

You can find more information about *Accepted Manuscripts* in the [Information for Authors](#).

Please note that technical editing may introduce minor changes to the text and/or graphics, which may alter content. The journal's standard [Terms & Conditions](#) and the [Ethical guidelines](#) still apply. In no event shall the Royal Society of Chemistry be held responsible for any errors or omissions in this *Accepted Manuscript* or any consequences arising from the use of any information it contains.

ARTICLE

A comparative study of Hispano-Moorish and Italian Renaissance lustred majolicas by using X-ray absorption spectroscopy.

Cite this: DOI: 10.1039/x0xx00000x

Received 00th January 2012,
Accepted 00th January 2012

DOI: 10.1039/x0xx00000x

www.rsc.org/

G. Padeletti^{a†}, C. Guglieri Rodriguez^b, P. Fermo^c, L. Olivi^b

Lustre is characterized by a heterogeneous metal-glassy nano-composite film, some hundreds nanometers thick. Silver and copper nanoparticles are dispersed within the outermost layers of the glaze, conferring to the whole materials peculiar optical properties. Even if numerous studies have been carried out [1-17], many questions regarding the chemical composition, the mechanism of metal reduction and the optical properties of lustre remain still open. Synchrotron radiation techniques are suitable for detailed studies on metal-glassy nano-composites [18-21]. For example, X-ray absorption fine structure spectroscopy (EXAFS) can provide useful information on oxidized phases or atomic clusters dispersed in an amorphous medium, otherwise not achievable with diffraction techniques.

In this work, we try to get information on the chemical state and local environment of metal atoms in the lustre and in the blue pigment, in order to achieve a better understanding of the reduction mechanism of different metals here present and the manufacturing techniques related to different productions (Hispano-Moorish and Italian Renaissance lustred majolicas). In particular, different samples characterized by lustre and blue decorations only, produced in Spain and in central Italy in XIV-XV cent., are compared

recipes and techniques for decorating ceramic objects. Mastro Giorgio Andreoli da Gubbio was the most important artist in this field, whose works can be found in the most important Museums of the world and are very well known in the antique trade market, as well [22-24]. His fame is due to the fact that optimising the lustre technique, he obtained outstanding results, that were not possible to replicate at his time and at present. He was specialised mainly in two kinds of reflects: an intense golden-yellow and a ruby-red colour, but the original recipes and technological procedures used at that time, were and remained a secret after his death and until today.

In the specific case of the Renaissance period, information on the majolica production technology were passed on by the Knight Cipriano Piccolpasso from Casteldurante, who wrote a treatise entitled "The three books on the art of the Potter" (1558). Anyway, the information reported by Piccolpasso could not be entirely correct, due to the aforementioned reasons, regarding the secrecy. Referring to his information, the objects were obtained in the desired form and fired in a first step at 1000 °C. Once cooked and cooled down, the object was immersed in the glaze constituted by sand, potassium carbonate, salts and oxides, such as lead and tin oxides, finely grinded and mixed with water. After drying in air, it was possible to decorate the glazed surface by using very soft brushes, made by bristle of goat, and, sometimes, for very fine details, whiskers of cats and mice, too. After that, sprayed with a transparent paint, the object underwent a second firing at 900 °C. At the end of this process, the object was complete.

Introduction

Lustre was one of the most sophisticated technique for the decoration of majolicas during the Renaissance period. Lustre consists of a thin metallic film containing silver, copper and other substances, like iron oxide and cinnabar, applied in a reducing atmosphere on a previously glazed ceramic. In this way, beautiful iridescent reflections of different colours (in particular gold and ruby-red) are obtained [1-17]. The characterisation and the study of lustre decorated majolicas is of great interest for archaeologists and scientists, today offering possibilities to produce pottery with outstanding decoration, following ancient examples, since nowadays artisans are interested in the reproduction of the ancient recipes and procedures. Lustre technique developed in Iraq and then spread to Egypt, Persia and Spain, following the expansion of the Arabian culture during the Medieval time. From Spain (Valencia, Manises and Malaga), lustre was introduced in the Italian peninsula, mostly in Central Italy where it was used to decorate the most beautiful majolicas. Gubbio and Deruta, located in the Umbria region, were important centres for this activity. It has to be pointed out that the Italian artisans developed their own style, for the decorative motifs, as well as for what concerns the metallic colours obtained. For this reason, the local artisans became keepers of refined and secret

1 However, if we refer to lustre, another step was required to
2 achieve the result of producing reflections and iridescences on
3 majolica. Ancient documentation indicates that the lustre was
4 obtained using a mixture of copper and silver salts, clays, ochre
5 and other optional substances, dissolved or dispersed in
6 vinegar, firing it in a reducing atmosphere at about 600 °C, in
7 special kilns made for this purpose, where probably it was
8 easier to control both the temperature and the atmosphere.

9 Lustre decoration in Italian and Hispano-Moorish majolicas has
10 been characterized by numerous analytical techniques. Today it
11 is well known that the lustre films resulted to be formed by
12 copper and silver clusters of nanometric dimension. The colour
13 and the properties of the lustre films depend on the elemental
14 composition of the impasto applied on the ceramic surface, as
15 well as on other factors like the metallic nanoclusters
16 dimension, determined by the firing conditions, the underlying
17 glaze composition and the procedures used [1-9]. Regarding
18 possible differences between both productions, it has been
19 found that Italian artisans added also bismuth to the impasto for
20 preparing the lustre, probably in order to keep down the cost. In
21 fact the cosalite phase ($\text{Pb}_2\text{Bi}_2\text{S}_5$) has been disclosed in the
22 Italian lustres and it can be considered as a marker which
23 allows us to attribute an object of uncertain provenance to the
24 Italian production [25-30].

25 In order to get a deeper knowledge of the differences between
26 the two different productions, X-ray absorption spectroscopy
27 (XAS) is a powerful tool allowing the determination of the
28 local environment around a selected atomic species. To date,
29 some studies have been carried by XAS on gold and red lustre
30 both of Italian and Hispanic provenance [18,19]. Even if the
31 oxidation state of copper and silver has been studied
32 extensively, blue decorations on lustre samples have not yet
33 been investigated in depth.

34 In this work, a XAS study has been carried on to get
35 information on the chemical state and on the local environment
36 of metal atoms in the glaze, lustre and blue pigment. For this
37 reason, samples produced in Spain and in central Italy in XIV-
38 XV centuries were compared, with the aim to achieve also a
39 better understanding of the technological process and materials
40 used in different productions.

41 Experimental

42 Two samples have been chosen to investigate possible
43 differences in the coordination state and local environment of
44 metal atoms constituting the blue pigment and the lustre in
45 Italian and Hispano-Moorish productions. The sample L19 is
46 representing a typical Italian Renaissance production, from
47 Central Italy, and LIM1 is representing a typical example of
48 Hispano-Moorish lustre. Both fragments are in very good
49 conservation state, never restored or treated. The two samples
50 were given us by Gubbio Town Council Museum and classified
51 by expert as original shards. In particular, both shards were
52 already the objects of archaeometric investigation [3, 5, 7, 25,
53 26]. XAS measurements were performed on XAFS beamline,

installed on a bending magnet source, at Elettra Sincrotrone
Trieste [31]. The storage ring energy was operated at 2.4 GeV
with a ring current of 159 mA. A Si (111) double-crystal
monochromator was used to monochromatize the white beam,
and higher harmonics were rejected by detuning the Bragg
angle of the second crystal. The beam size was set at $1 \times 1 \text{ mm}^2$
and the photon flux was about 10^{10} photons/s. All spectra were
collected at Fluorescence mode, with a Silicon Drift Detector.

In addition several references (CoO , Co_3O_4 , NiO metal Cu,
 CuO and Cu_2O) were measured in transmission mode. The
spectra were recorded at both the X-ray Absorption Near Edge
Structure (XANES) and the Extended X-Ray Absorption Fine
Structure (EXAFS) regions.

The analysis were performed according to standard procedures
[32]. XAS spectra were normalized, after background
subtraction, to the averaged absorption coefficient at high
energy. EXAFS signals (k) were extracted from the spectra by
using the Athena software [33], removing the background by a
cubic spline polynomial fitting and normalising the magnitude
of the oscillations to the edge jump. The corresponding
pseudoradial distribution function around the photoabsorbing
atom has been obtained by performing the Fourier transform,
FT (using a sine window). The fitting to the experimental data
was carried out in both R-space and q-space, by using the
programme Artemis, also within the IFEFFIT package [33].

The study was focused on Hispano-Moorish LIM1 and Italian
L19 samples dated back to XIV-XV cent. XANES and EXAFS
spectra were recorded at the Co K-edge (7709 eV), Ni K-edge
(8333 eV) and Cu K-edge (8979 eV) in the blue pigmented
regions of the pottery, and at the Cu K-edge at the lustre. The
FT of the EXAFS signals were filtered in the interval $k = 2.5 \leq$
 $k \leq 11.7 \text{ \AA}^{-1}$, $k = 2.3 \leq k \leq 8.8 \text{ \AA}^{-1}$ and $k = 2.5 \leq k \leq 10.7 \text{ \AA}^{-1}$
for the Co, Ni and Cu K-edge respectively.

SEM-EDX analyses were acquired on thin sections obtained
starting from cross-sections prepared embedding the shards into
a suitable resin. The instrument used was a Hitachi TM1000
equipped with an energy dispersive X-ray Spectrometer
(Oxford Instruments SwiftED).

42 Results and discussion

43 1. SEM measures on the Blue Pigment

The SEM images acquired on the two thin sections of the
samples LIM1 and L19, are shown in Fig. 1. At a first glance it
is evident that the Hispano-Moorish sample shows a glaze
which is more homogeneous with respects to the Italian one.
Furthermore the glaze thickness in LIM1 is lower (about 100
 μm) with respect to that one of the Italian lustre (between 160
and 180 μm). EDS analyses (not shown) evidenced the
presence of iron, cobalt and nickel in the blue parts, in
accordance with what previously observed for the blue colour
[3].

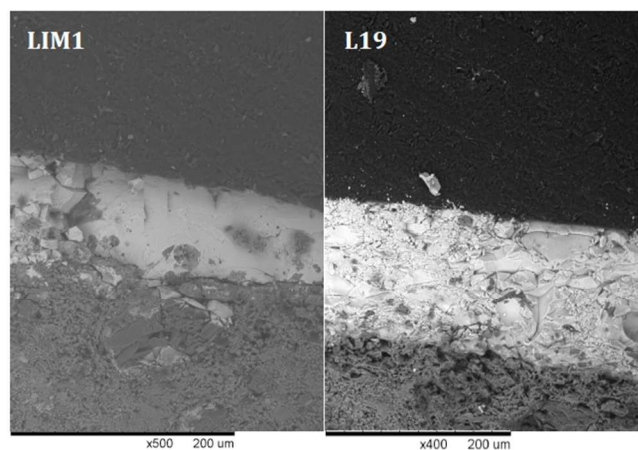


FIG. 1: SEM images acquired on thin sections corresponding to the analysed samples LIM1 and L19.

2. XAS study on the Blue Pigment

2.1 Co K-edge

The Co K-edge XANES spectra are shown in Fig.2, together with some references, as indicated in the caption.

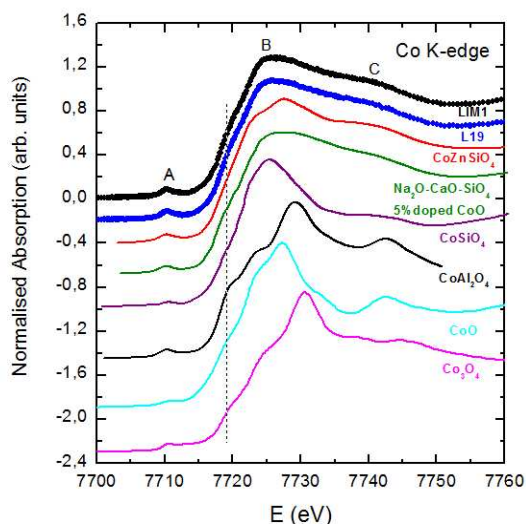


FIG. 2: Comparison of Co K-edge XANES spectra of the blue pigments in L19 and LIM1 samples, and CoZnSiO_4 , $\text{Na}_2\text{O-CaO-4SiO}_4$ 5% CoO doped, CoSiO_4 , CoAl_2O_4 , CoO , Co_3O_4 spectra as references.

LIM1 and L19 spectra present the same shape. The main characteristics are a sharp pre-peak, labelled like A, and a broad white line, B, followed by a hump-like feature C. The low detailed structures indicate the poor crystalline quality of the Co environment. The FT of the EXAFS signals is shown in Fig.3. For both cases it consists of only a peak at 1.6 Å,

corresponding to the first coordination shell. Due to the low crystallinity of the samples, further peaks are not found. The signals were fitted to a first Co-O shell. The interatomic distances, coordination numbers and Debye-Waller factors obtained from the best fits, are reported in Table I. The fitting parameter R-factor (not shown) demonstrated the quality of the fits.

The energy edge for both L19 and LIM1 samples is at 7718 eV, corresponding to a Co^{2+} oxidation state. Previous results for similar samples [34] suggested the presence of Co_3O_4 and CoO in the blue pigment. Since Co_3O_4 is a mixed valence compound, containing Co^{2+} and Co^{3+} ions, it does not seem to be significantly present in any of the analysed samples. On the other hand, we can not exclude the presence of CoO . However, the comparison of the XANES profiles (see Fig.2) indicates that the main contribution to the L19 and LIM1 spectra can not arise from that compound. This is clear for the lack of the pre-peak A and for the shifted position of peak B. Indeed, the relatively intense pre-peak A indicates that Co^{2+} is in tetrahedral sites (or in a highly distorted octahedron). That would be expected, since previous studies about the blue pigmenting properties of Co ions had already established that the blue colour is due to tetrahedral Co^{2+} compounds [35]. In Fig.2 some crystalline references of several Co^{2+} compounds frequently used for pigmentation have been included: CoZnSiO_4 [36], CoAl_2O_4 and CoSiO_3 [37]. For further information, we have added the spectrum of $\text{Na}_2\text{O-CaO-4SiO}_4$ 5% CoO doped (labelled as NaCa) [36]. In CoZnSiO_4 , CoAl_2O_4 and NaCa the Co ions are located at tetrahedral sites, while in CoSiO_3 the structure around Co corresponds to a distorted octahedron. The spectral profiles of L19 and LIM1 samples look very similar to those of CoZnSiO_4 , and particularly to that one of NaCa. The similarity of the spectra strongly suggests that Co ions are in an analogous tetrahedral compound. On the other hand, a simultaneous contribution of CoAl_2O_4 and CoSiO_3 could lead to a similar spectral shape, which is reasonable, since the presence of Si and Al in both samples has been previously proved [30].

The interatomic distances and coordination numbers obtained from the best fit of the EXAFS signals (Table.I) coincide with previous results obtained for systems with Co in tetrahedral coordination [34, 38]. In the case of LIM1 the Co-O bond distances are slightly bigger, but still comparable to the reported results [39]. This increase could be also due to a higher contribution of Co^{2+} ions in octahedral sites (nominally larger than those in tetrahedral sites) that would be higher in the Hispano-Moorish LIM1 than in the Italian L19 sample. It is important to note that these findings are different from what was found by other authors [34], that studied old Sicilian shards (from Caltagirone site), and in which the blue pigments were found to be related to CoO and Co_3O_4 . In any case, our findings do not confirm important differences between the cobalt compounds forming the blue pigments under investigation, indicating an affinity between Hispano-Moorish and Italians for what concerns the materials used in the ceramic production. Probably, this fact was determined and facilitated by the active commercial exchanges and contacts between them, at that time.

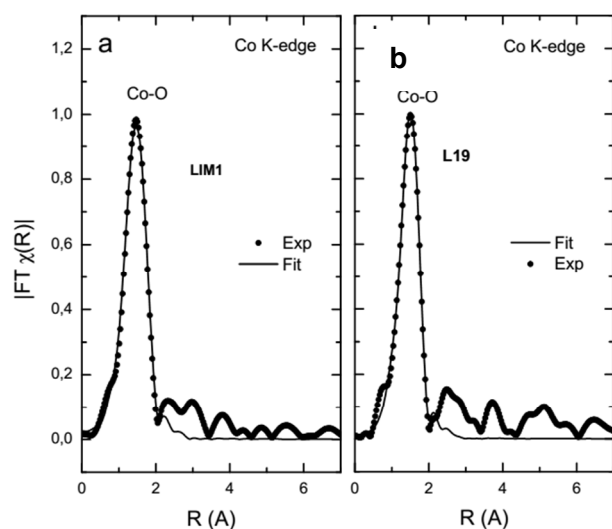


FIG. 3: Moduli of the Fourier Transform (dots= experimental signals; line= fits) for the blue pigment in a) LIM1 and b) L19 samples at the Co K-edge of the first coordination shell, Fitting range: $1 \leq R \leq 2$

Sample	Coord.	N	r (Å)	σ^2 (Å ²)
L19	Co-O	3.8 ± 0.1	1.97 ± 0.01	0.005 ± 0.001
LIM1	Co-O	3.5 ± 0.4	2.1 ± 0.01	0.006 ± 0.002

TABLE I: Best fit parameters obtained from the analysis of the first shell contribution of the Co K-edge EXAFS spectra: N coordination number; r distances; σ^2 Debye-Waller factor. Filtering range: $2.5 \leq k \leq 11.7 \text{ \AA}^{-1}$. Fitting range: $1 \leq R \leq 2$

2.1 Ni K-edge

The Ni K-edge XANES spectra are shown in Fig.4. The spectrum of NiO is also included. As expected the samples are not crystalline and so their spectral shapes are not very sharp or defined. The FT of the EXAFS signals are shown in Fig.5, and the interatomic distances, coordination numbers and Debye-Waller factors obtained from the best fits, are reported in Table II. The fitting parameter R-factor (not shown) demonstrated the quality of the fits.

The XANES signals are again identical for both samples. Considering the position of the energy edge at 8344 eV and the spectral features, it is most likely to correspond to an amorphous NiO. The fits of the EXAFS signals (Fig.5) support this, as the obtained coordination numbers and interatomic distances clearly match those of NiO (Table. II). In this case, the EXAFS signals are different for the Italian and the Hispano-Moorish samples. While the module of the FT of the L19 spectrum displays only a peak,

corresponding to the first NiO bonds, and a second peak is hinted, in the LIM1 that second peak at 2.4 \AA is enhanced. This second feature can be attributed to Ni-Ni bonds, hence, in the LIM1 sample the NiO structure is ordered up to the second coordination shell (Ni-O-Ni).

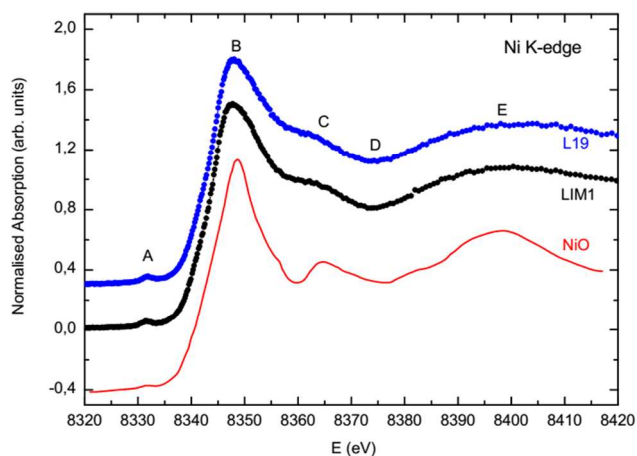


FIG. 4: Ni K-edge XANES spectra of the L19 and LIM1 samples, and NiO reference

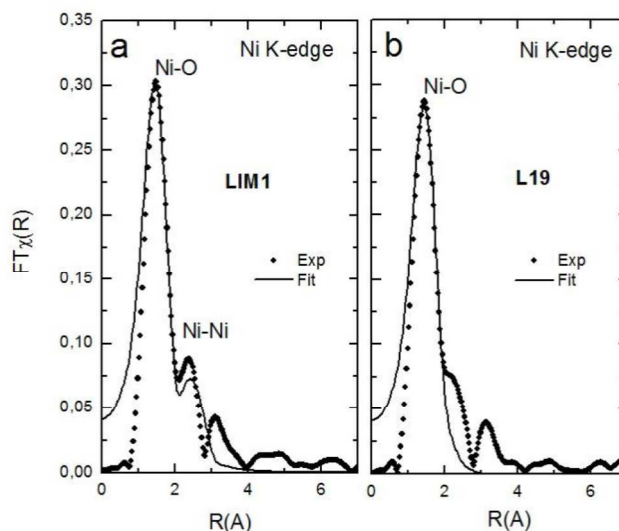


FIG. 5: Moduli of the Fourier Transform (dots for experimental signals, line for fits) for the blue pigment in a) LIM1 and b) L19 samples at the Ni K-edge of the first coordination shell, Fitting range: $1 \text{ \AA} \leq R \text{ \AA} \leq 2.8$ and $1 \text{ \AA} \leq R \text{ \AA} \leq 2.1$, respectively

Sample	Coordin	N	R (Å)	σ^2 (Å ²)
NiO	Ni-O	6	2.08	
	Ni-Ni	12	2.95	
LIM1	Ni-O	5.3 ± 1.0	2.06 ± 0.01	0.007 ± 0.007
	Ni-Ni	10.5 ± 1.0	3.06 ± 0.04	0.029 ± 0.006
L19	Ni-O	5.3 ± 1.0	2.04 ± 0.03	0.011 ± 0.008

TABLE II: Best fit parameters at the Ni K-edge: N coordination number; r distances; σ^2 Debye-Waller factor. Filtering range: $1 \leq k \leq 8.7 \text{ \AA}^{-1}$. For L19 the analysis correspond to the first shell (Fitting range: $1 \leq R \leq 2.1$). For LIM1 the best results are obtained by including a second shell (Fitting range: $1 \leq R \leq 2.8$)

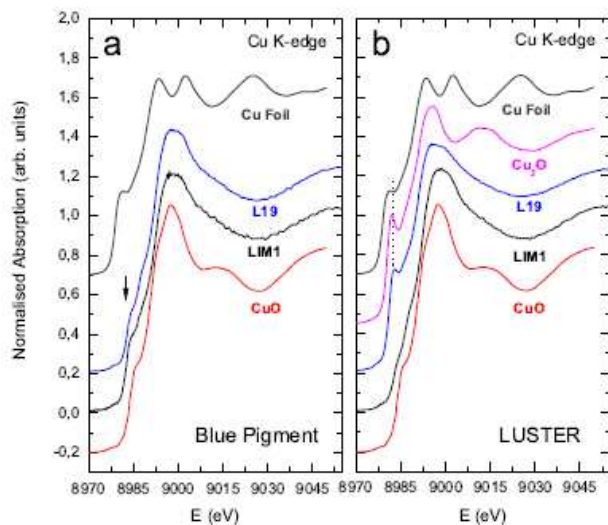


FIG. 6: Cu K-edge XANES spectra of CuO, Cu₂O, metallic Cu foil and of LIM1 and L19 on the blue pigment (a) and on the lustre (b).

2.1 Cu K-edge

Finally, the Cu K-edge signals was measured on the blue pigments present on both samples, that in some parts were covered with lustre and the results are presented in Fig. 6a. CuO, Cu₂O and metallic Cu references are added for comparison. The spectral profiles and the position of the edge indicate that copper is close to the Cu²⁺ oxidised form. However, the small modifications of the edge and pre-edge could entail a started reduction of the Cu ions (similar structures in reduced CuO have been reported by several author [40]). The EXAFS signals and the magnitude of the FT show that the Cu environment present short range order in all cases,

and just the contribution of the first Cu-O bonds is appreciable. The EXAFS contribution of this shell was isolated by Fourier filtering in the range from $0.8 \leq R \leq 2 \text{ \AA}$, and then analysed. The results of the fits are shown in Fig. 7.a and the best parameters are summarized in Table III. As expected, the interatomic Cu-O resulting distances are similar to the nominal values in CuO.

3. XAS study at the Lustre

The study of the lustre was focused on the Cu K-edge. XANES spectra recorded at lustre are shown in Fig. 6.b. The EXAFS signals were also measured and the moduli of the FT consist only in one peak; just the contribution of the first Cu-O bonds is appreciable. The EXAFS contribution of this shell was isolated by Fourier filtering in the range from $0.8 \leq R \leq 2 \text{ \AA}$. The filtered signals and the results of the fits are shown in Fig. 7.b and the best parameters are summarized in Table III.

The XANES spectra registered in the lustred regions of both samples display significant differences: the L19 XANES spectrum presents the characteristic pre-peak and energy edge (8981 eV) of Cu₂O. On the other hand, the spectrum of LIM1 does not show the pre-peak, and the position of the energy edge, at 8983 eV, is in this case closer to CuO. Anyhow, the differences in the edge indicate as well a started reduction of the Cu ions.

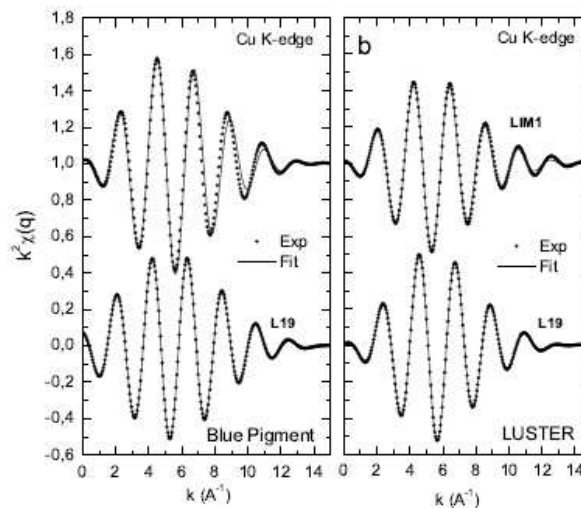


FIG. 7: k^2 -weighted filtered EXAFS data (dots) and best fit obtained with parameters included in Table III (line) of the a) blue pigment and b) lustre in LIM1 and L19 samples, respectively.

In agreement with the previous discussion, the obtained Cu-O interatomic distance found in the L19 sample is the same of

Cu₂O, while in the LIM1 sample the result matches that one of CuO.

Sample	Coordin.	N	r (Å)	σ^2 (Å ²)
CuO	Cu-O	4	1.95	
Cu ₂ O	Cu-O	2	1.84	
LIM1 blue	Cu-O	3.5 ± 0.4	1.92 ± 0.01	0.006 ± 0.002
L19 blue	Cu-O	3.8 ± 0.1	1.93 ± 0.01	0.001 ± 0.002
LIM1 lustre	Cu-O	3.5 ± 0.4	1.92 ± 0.01	0.006 ± 0.002
L19 lustre	Cu-O	3.2 ± 0.1	1.84 ± 0.01	0.005 ± 0.003

TABLE III: Best fit parameters obtained from the analysis of the first shell contribution of the Cu K-edge EXAFS spectra: N coordination number; r interatomic distances; σ^2 Debye-Waller factor. Filtering range: $2.5 \leq k \leq 10.7 \text{ \AA}^{-1}$. Fitting range: $0.8 \leq R \leq 2$.

Our results for the Italian L19 sample are in agreement with previous works concerning similar samples from the Italian Renaissance [41]. Those works reported the presence of metallic Cu in the very near surface region of the lustre; however, in our case, when XAS measurement were performed in Fluorescence mode, the results pointed out the presence of Cu₂O. The different outcome depends to the deeper sampling probing achieved by the fluorescence mode (about 30 μm), not so sensible to the near surface zone.. At the first step of the formation of lustre, copper ions would migrate from the initial lustre paste to the glaze, and after the ion penetration into the glaze. A reduction to metal Cu nanoparticles is expected, as a consequence of the reductive atmosphere created in the kiln. Therefore, the amount of reduced metallic copper would be distributed in the region near the surface and at the deeper regions the Cu ions would be mostly in oxidized form. However, the results of the Hispano-Moorish LIM1 sample indicate a less reduced state of Cu ions, similar to what found for Cu ions in the blue part. Considering all, it seems feasible that the dispersion of Cu ions into the glaze occurred at a different efficiency for the L19 and the LIM1 samples, respectively. In this case, an interpretation could be made considering the use of different technological procedures generating different efficiency in the reducing phase and consequently generating copper ions in different oxidation states.

In Tab. IV the chemical composition of the analysed shards is reported; it is possible to note that they present great differences as concerns Cu/Ag ratios and the chemical composition certainly influences the reduction process. As well, the bismuth

reported in table IV confirm its use only in the Italian production [25-30], and it is not possible to generalize its use as reducing agent, since in Hispano-Moorish production it is not present at all, and in the Italian production is found as cosalite. In this compound the Bi oxidation state is +3, then, it is not present in its oxidized form, which would be indicative of its reducing activity.

Sample	Cu/Ag	Ag/Cu	Bi/Ag
L19	9,17*	0,11	5.6**
LIM1	89,90***	0,011	-- ***

Table IV: Elemental composition by ETAAS: *in [3]; ** in [25]; ***in [26]

Conclusions

In this work two lustred majolica shards, from Hispano-Moorish (LIM1) and Italian (L19) productions, were studied in two different regions: on the blue pigment and on the lustre.

On the blue pigment XAS spectra were measured at the Co, Ni and Cu K-edge. Concerning the Co, for both production the XANES spectra pointed out the poor crystallinity of the Co environment as well as a main contribution of Co²⁺ ions at tetrahedral sites. Besides, the analysis of the EXAFS signals show values of Co-O interatomic distances in agreement with the conclusions of the XANES. In the case of the Hispano-Moorish LIM1 sample, those distances are slightly higher, indicating a higher contribution of Co²⁺ at octahedral sites. The blue pigmentation could be due to a compound analogous to NaCa or to the contribution of both CoAl₂O₄ and CoSiO₃. Ni is present as NiO but some differences arise between the two sample. In fact, despite the sample is amorphous, as expected, in LIM1 the NiO structure is ordered up to the second coordination shell (Ni-O-Ni). The Cu spectra in the blue parts are quite similar, and indicate that Cu is close to Cu⁺², even though it is possible to observe, for both samples, an edge modification that suggest a started reduction of the Cu ions.

For what refer to lustre, significant differences have been observed when the Cu XANES spectra are compared: L19 has a behaviour matching Cu₂O. The behavior of LIM1 matches CuO, indicating, for this sample a lower reduction degree. In this case, an interpretation could be made on the base of the different technological processes used, producing at last, copper ions in different oxidation states.

Acknowledgements

M. Hunault, (Université Pierre et Marie Curie - Paris 6), Paris), J. Perez-Arategui (University of Zaragoza), A. Longo (ISMN-CNR, Palermo) and M.P. Casaletto (ISMN-CNR, Palermo) are

1 kindly acknowledged for helpful discussions. Gubbio Town
 2 Council is kindly acknowledged for having supplied the
 3 analysed samples
 4
 5
 6
 7

Notes and references

8 ^a ISMN-CNR Area della Ricerca Roma1, via Salaria Km. 29,5, 00015
 9 Monterotondo (RM), Italy.

10 ^b Elettra Sicrotrone Trieste, Strada Statale 14 - km 163,5 in AREA
 11 Science Park, 34149 Basovizza, Trieste, Italy., .

12 ^c Dip. Chimica, Università di Milano, Via Golgi, 19, 20133 Milano, Italy.

13 † contacting author: giuseppina.padeletti@cnr.it

- 14
 15
 16
 17
 18 1 I. Borgia, B. Brunetti, I. Mariani, A. Sgamellotti, F. Cariati, P.
 19 Fermo, M. Mellini, C. Viti, G. Padeletti, *Applied Surface Science*
 20 **185**, 206, (2002)
 21 2. P. Fermo, F. Cariati, C. Cipriani, M. Canetti, G. Padeletti, B. Brunetti,
 22 A. Sgamellotti, *Applied Surface Science* **185**, 309 (2002)
 23 3 G. Padeletti, P. Fermo, *Applied Physics A*, **76**, 515, (2003)
 24 4 G. Padeletti, P. Fermo, *Applied Physics A*, **79**, 241, (2004).
 25 5 A. Galli, M. Martini, E. Sibilia, G. Padeletti, P. Fermo, *Applied*
 26 *Physics A*, **79**, 293, (2004)
 27 6 G. Padeletti, P. Fermo, *Techné*, **20**, 35, 2004
 28 7 S. Berthier, G. Padeletti, P. Fermo, A. Bouquillon, M. Aucouturier, E.
 29 Charron, V. Reillon, *Appl. Phys. A*, **83**, 573, (2006)
 30 8 G. Padeletti, P. Fermo, *J. of Nanoscience and Nanotechnology*, **12**,
 31 8764, (2012)
 32 9 P. Fermo and G. Padeletti, *Applied Physics A*, **113**, 825, (2013)
 33 10 T. Pradell, R. S. Pavlov, P. C. Gutiérrez, A. Climent-Font and J.
 34 Molera, *J. Appl. Phys.* **112**, 054307 (2012);
 35 11 G-. Molina, M. S. Tite, J. Molera, A. Climent-Font, T. Pradell,
 36 *Journal of the European Ceramic Society*, **34**, 2563, (2014)
 37 12 T. Pradell, J. Molera, C. Bayés, P. Roura, *Applied Physics A*, **83** 203,
 38 (2006)
 39 13 T. Pradell, J. Molera, A.D. Smith and M.S. Tite, *Journal of*
 40 *Archaeological Sciences*, **35**, 1201, (2008)
 41 14 J. Pérez-Arategui, J. Molera, A. Larrea, T Pradell, M Vendrell-Saz, I
 42 Borgia, B. G. Brunetti, F. Cariati, P. Fermo, M. Mellini, A.
 43 Sgamellotti and C. Viti, *J. Am. Ceram. Soc.* **84**, 442, (2001)
 44 15 J. Roqué, J. Molera, J. Pérez-Arategui, C. Calabuig, J. Portillo and
 45 M. Vendrell-Saz, *Archaeometry*, **49**, 511, (2007)
 46 16 J Pérez-Arategui, A. Larrea, *Trends in Analytical Chemistry*, **22**,
 47 327, (2003)
 48 17 P. Colomban, *J. Nano Res.* **8**, 109, 2009
 49 18 S. Padovani, D. Puzzovio, C. Sada, P. Mazzoldi, I. Borgia, A.
 50 Sgamellotti, B.G. Brunetti, L. Cartechini, F. D'Acapito, C. Maurizio,
 51 F. Shokoui, P. Oliyai, J. Rahighi, M. Lamehi-Rachti, E. Pantos, *Appl.*
 52 *Phys. A* **83**, 521 (2006)
 53 19 A. Smith, T. Pradell, J. Roqué, J. Molera, M. Vendrell-Saz, A.J.
 54 Dent, E. Pantos, *J. Non Cryst. Solids*, **352**, 5353, (2006)
 55 20 F. Gonella, P. Mazzoldi, *Handbook of Nanostructured Materials and*
 56 *Nanotechnology*, Vol. 4, ed. by H.S. Nalwa (Academic, San Diego,
 57 2000)

- 21 U. Kreibig, M. Vollmer, "Optical properties of Metal Clusters"
 (Springer, Berlin, 1995)
 22 G. Padeletti, G. M. Ingo, A. Bouquillon, S. Pages-Camagna,
 M. Aucouturier, S. Roehrs, P. Fermo, *Appl. Phys. A*, **83**, 475, (2006)
 23 G. Padeletti, *Ceramics Art and Perspection*, **64**, 44, (2006)
 24 G. Padeletti, G.M. Ingo, A. Bouquillon, M. Aucouturier, M.L. de
 Rochebrune, F. Barbe, on "Mastro Giorgio da Gubbio - Art, Science
 and Technology of Lusted Majolicas" - Volumnia Ed., 2013, pag
 151-174
 25 G. Padeletti, P. Fermo, *Applied Physics A*, **77**, 125, (2003)
 26 G. Padeletti, P. Fermo, *Applied Physics A*, **79**, 277, (2004)
 27 D. Cabanne, A. Bouquillon, M. Aucouturier, X. Dector, G. Padeletti,
Applied Physics A, **92**, 11, (2008)
 28 G. Padeletti, P. Fermo, A. Bouquillon, M. Aucouturier, F. Barbe,
Applied Physics A, **100**, 747, (2010)
 29 G. Padeletti, P. Fermo, *Applied Physics A*, **100**, 771, (2010)
 30 G. Padeletti, P. Fermo, A. Bouquillon • M. Aucouturier, F. Barbe, on
 "Mastro Giorgio da Gubbio - Art, Science and Technology of Lusted
 Majolicas"- Volumnia Ed., 2013, pag 175-196
 31 A. Di Cicco, G. Aquilanti, M. Minicucci, E. Principi, N. Novello, A.
 Cognigni, and L. Olivi, *Journal of Physics: Conference Series* **190**
 012043 (2009)
 32 G. Bunker, *Introduction to XAFS* (Cambridge University Press,
 2010)
 33 B. Ravel and M. Newville, *J. Synchr. Radiat.* **12**, 537 (2005)
 34 D. Barilaro, V. Crupi, S. Interdonato, D. Majolino, V. Venuti, G.
 Barone, M.F. la Russa and F. Bardelli, *Appl. Phys. A* **92** 91, (2008)
 35 T. Minami and S. Ghosh, *Current Science* **78**, 892, (2000)
 36 M. Hunault, G. Calas, L. Galois, G. Lelong and M. Newville, *J. Am.*
Ceram. Soc. **97** 60, (2014)
 37 H. Wang et al. *Journal of Catalysis* **300**, 91 (2013)
 38 L. Wang and C. Wang, *J. Anal. At. Spectrom.* **26** 1796, (2011)
 39 M.O. Figueiredo, T.P. Silva, J.P. Veiga, M.I. Prudencio, M.I. Dias,
 M.A. Matos and A.M. Pais, on "LASMIC & IMRC 2009-Selected
 papers 2010", 84-88 (2010)
 40 J.Y. Kim, J.A. Rodriguez, J.C. Hanson, A.I. Frenkel and P.L. Lee, *J.*
Am. Chem. Soc. **125** 10685, (2003)
 41 S. Padovani, I. Borgia, B. Brunetti, A. Sgamellotti, A. Giulivi, F.
 D'Acapito, P. Mazzoldi, C. Sada and G. Battaglin., *Appl. Phys. A*, **79**,
 229, (2004)